

Wetting transitions of Ne

M. J. Bojan^{1,4}, G. Stan², S. Curtarolo^{2,3}, W. A. Steele¹, and M. W. Cole²

¹*Department of Chemistry, Penn State University, University Park, PA 16802, USA*

² *Department of Physics, Penn State University, University Park, PA 16802, USA*

³*University of Padua, Physics Department, Padua, Italy*

⁴e-mail address: mjb@chem.psu.edu

phone: (814)865-2895, fax: (814)863-5319

(January 5, 2018)

Abstract

We report studies of the wetting behavior of Ne on very weakly attractive surfaces, carried out with the Grand Canonical Monte Carlo method. The Ne-Ne interaction was taken to be of Lennard-Jones form, while the Ne-surface interaction was derived from an ab initio calculation of Chizmeshya *et al.* Nonwetting behavior was found for Li, Rb, and Cs in the temperature regime explored (i.e., $T < 42$ K). Drying behavior was manifested in a depleted fluid density near the Cs surface. In contrast, for the case of Mg (a more attractive potential) a prewetting transition was found near $T = 28$ K. This temperature was found to shift slightly when a corrugated potential was used instead of a uniform potential. The isotherm shape and the density profiles did not differ qualitatively between these cases.

PACS numbers: 64.70.Fx, 68.35.Rh, 68.45.Gd, 82.20.Wt

I. INTRODUCTION

During the last few years there has developed great interest in the existence and nature of wetting transitions of adsorbed simple gases [1]. By “wetting” we mean complete wetting, i.e., the formation of a film with thickness that diverges as the pressure approaches saturation. The problem of wetting has long been interpreted qualitatively in terms of the relative magnitudes of the cohesive energy of the adsorbate and the adhesive energy binding the adsorbate to the substrate [2]. If the latter is small compared to the former, then a simple surface energy argument implies that the gas does not wet the surface at low temperature (T). Some 20 years ago it was argued that such a gas will undergo a wetting transition (of some kind) as T is increased to the critical temperature [3,4]. The argument has been made both qualitatively, in terms of general arguments involving entropy and/or surface tension, and quantitatively using several varieties of model calculations.

Experimental evidence for such transitions was initially slow to appear. In 1992, the first example of a prewetting transition was found, for the case of He adsorption on Cs [5,6]. Prewetting is a first order transition manifested by a coverage jump as a function of vapor pressure (P). This transition had been predicted to occur [7] as a consequence of the extremely weak attraction; the well depth D of the He attraction to a Cs surface (0.6 meV) is even smaller than the well depth ϵ of the interaction between two He atoms (0.95 meV)! These observations were followed by qualitatively similar evidence (from theory and experiment) of prewetting transitions of H_2 films on Rb and Cs [8,9]. These findings lead one to ask about homologous systems, such as Ne films on alkali metals. There are several simple ways to appraise a given adsorption system and estimate its wetting properties. If one evaluates the dimensionless ratio $D^* = D/\epsilon$, one finds that D^* is smaller for Ne on Cs than for any other adsorption system in this class; see Table I [10,11]. This weak relative attraction implies a nonwetting situation at low T . Further support for this expectation was obtained from a simple model [12] which compares the cost (surface tension) of forming a thick film with the benefit (the gas-surface attractive interaction). This approach gives the following relationship which is satisfied at the wetting temperature (T_w)

$$(\rho_l - \rho_v)I_V = 2\gamma \quad (1)$$

$$I_V = - \int_{z_{min}}^{\infty} dz V(z) \quad (2)$$

where ρ_l and ρ_v are the densities of the adsorbate liquid and vapor at coexistence, γ is the surface tension of the liquid, and z_{min} is the equilibrium distance of the potential. This model predicts that wetting transitions for Ne/Rb and Ne/Cs should occur within a few per cent of the Ne critical temperature ($T_c = 44.4$ K). Very recently, experimental support for that prediction was found in quartz microbalance measurements on these surfaces. The data of Hess *et al.* [14] imply that Ne undergoes a wetting transition within 2% of T_c on Rb and that it undergoes a drying transition on Cs. The latter is a unique observation, to the best of our knowledge. We note in passing that qualitatively similar prewetting transitions have been seen recently in Hg adsorption on Mo and sapphire surfaces [15,16].

These observations have led us to undertake computer simulation studies of Ne adsorption on various surfaces [17]. We have used the Grand Canonical Monte Carlo (gcmc) method, which assumes that the behavior of the Ne atoms is classical. The accuracy of this assumption for Ne in this temperature range has been demonstrated recently in detailed calculations of Johnson and coworkers [18]. We have assumed a Lennard-Jones interatomic interaction between the Ne atoms, which should be qualitatively adequate. Finally, we have considered two regimes of adsorption interaction. One set of calculations pertains to the ultraweakly adsorbing alkali metal surfaces. Our finding of nonwetting behavior is qualitatively consistent with the experimental results, within the limited regime of our study. The presence of critical fluctuations prevents us from approaching very close to T_c because there the correlation length exceeds the size of the periodically replicated unit cell on the surface (2.8 nm). The second set of calculations pertains to the case of Ne on much more attractive surfaces (e.g. Mg). There we find clearly defined prewetting transition behavior. That system has not yet been studied experimentally.

Our calculations are not the first simulation studies of the prewetting phenomenon. Previous studies by several groups on a model surface yielded prewetting transition behavior for an assumed model potential (Ar on CO₂) [19–21]. Curiously, previous and subsequent studies, by Nijmeijer, Sikkenk and coworkers, did not find that transition for a similar system [22–24]. Possible reasons for the discrepancy include the role of fluctuations and metastability, which are prominent and troublesome in most simulations of this problem. Also, while Nijmeijer and

coworkers used a very large system size in their simulations, their choice of the constant volume, constant temperature algorithm was not as well suited to the study of prewetting as the isobaric isothermal simulations used by Monson *et al* [19,20]. In our study, we are using the gcmc simulation technique, for which the chemical potential of the system is known. Although it is still possible to obtain metastable states in gcmc, we found the problem to be greater at higher temperatures and therefore were obliged to perform more extensive (longer) simulations in the metastable regions at high temperatures.

The outline of this paper is the following. Section 2 describes the potentials used as well as our simulation methods. Section 3 describes the results found for the ultraweakly adsorbing surfaces. Section 4 presents our results for more strongly adsorbing surfaces including the Ne/Mg case. These include analyses for the case of an assumed continuum substrate (translationally invariant potential) and a more realistic substrate (corrugated potential). Section 5 summarizes our results and describes other work and predictions which are relevant to this problem.

II. MODEL POTENTIALS AND MONTE CARLO SIMULATIONS

The Ne-Ne interaction used in this study is the well-known Lennard-Jones 12-6 potentials. Therefore, the results reported here are relevant to any classical inert gas as well as to a number of simple molecular gases for which such potentials are appropriate. Consequently, we can use energies reduced by k (units of K), remembering that $\epsilon_{Ne-Ne}/k=33.9$ K gives the correct reduced critical temperature $T_c^* = kT_{cr}/\epsilon_{gg}=1.31$ [25] for a Lennard-Jones gas. The cutoff distance used for the potential was rather large (5σ) since it has been noted previously [21] that a small cutoff gives different results for the fluid properties. For example, in the simulations of Finn and Monson [19], using a potential cutoff of 2.5σ gives a critical temperature, $T_c^* = 1.23$. Although we did not evaluate the critical temperature, the condensation pressures of Ne in our simulations agree with the vapor pressures as given by Lotfi *et al.* [26], whose work confirms the value of $T_c^* = 1.31$ for a Lennard-Jones fluid.

The gas-solid potential is derived from a model in which a gas atom interacts with the atoms in the solid via pairwise Lennard-Jones functions [27] and thus has a somewhat different form from that expected for gases interacting with a metal surface. Replacing the sums over the solid

atoms in planes parallel to the surface with integrals gives a gas-solid energy $U_{gs}(z)$ which is:

$$U_{gs}(z) = \epsilon_{1s} \sum_{j=0} \left[\frac{2}{3} \left(\frac{\sigma_{gs}}{z + jd} \right)^{10} - \frac{5}{3} \left(\frac{\sigma_{gs}}{z + jd} \right)^4 \right] + corr \quad (3)$$

where z is the perpendicular distance of the adsorbate atom from the surface, ϵ_{1s} is the well-depth, the sum has been truncated after $j = 3$, and $corr$ denotes a small correction term for interaction with the more distant planes. The relationship between the well-depth D for the interaction of an atom with the entire surface and ϵ_{1s} is $D \approx 1.2\epsilon_{1s}$ for the interplanar spacing chosen for this study [28]. σ_{gs} is the size parameter of the potential and was taken to be .501 nm; d is the distance between planes in the solid and has been set equal to .401 nm in this work. In particular, the relatively large values of σ_{gs} will give long-ranged potentials similar to those for the 9-3 functions used in the theoretical treatments of inert gases on alkali metals [10]. (See Fig. 1 for a comparison of these potentials along with the potential for the interaction of inert gases with CO₂.) The range of the potentials for atoms over alkali metal surfaces is particularly large due to the large decay lengths of the surface electronic charge in these systems [29].

Various well-depths were chosen for study, ranging from $D = 16.8 K$ to $120 K$ so that the transition from non-wetting to wetting behavior in these systems could be characterized. The studies by Finn and Monson [19], Fan and Monson [20], Sokołowski and Fischer [21] correspond to the relative well depth $D^* = 2.64$. The Dutch group (Nijmeijer, Sikkenk, *et al.* [22–24]) reported simulation results covering a wide range of D^* values similar to ours ($D^* \approx 0.5$ to 3.5), but they were not able to identify unambiguous prewetting transitions because their simulations were done in the canonical ensemble.

The application of the gcmc algorithm to the study of adsorption is now a well-known and extensively utilized technique [30–32]. The present and previous simulations of wetting systems determine adsorption isotherms by evaluating the average number of particles \bar{N} in a computer box for fixed values of box volume V , chemical potential μ and temperature T . The box has periodic boundary condition in two dimensions. At least one of the remaining two walls is the adsorbing surface, with the final wall being either a second adsorbing surface or a hard wall that serves only to keep the gas molecules in the box. The second of these options was used in the present work. Of course, this requires that these two walls be rather widely separated so the presence of the second wall has negligible influence on the wetting or adsorption properties of

the system. One method of monitoring this is to evaluate the local density of the fluid in the system. If the varying local densities observed in the regions near the walls are separated by a large region of constant density, one may reasonably argue that the adsorption is in contact with a phase having bulk properties. (It is this assumption that underlies nearly all simulations of physical adsorption.) Of course there is no assurance that the phase having constant density is the bulk equilibrium phase. For the simulations reported here, these two walls were separated by 7.5 nm; auxiliary simulations with both larger and smaller wall separations exhibited no observable dependence of the thermodynamic properties of the fluid near the wall upon distance in this range.

The chemical potential of an adsorbed phase is related to experimentally measurable quantities by equating it to μ for the bulk. If the bulk phase is an ideal gas, one can calculate the chemical potential from $kT \ln p$. However, this approximation fails rather badly for the pressures of interest in the present work, due to deviations from ideality in the bulk gas phase. For example, the leading term in the difference $\mu_{gas} - \mu_{id}$ for the real and the ideal gas at the same pressure is given by:

$$\frac{\mu_{gas} - \mu_{id}}{kT} = -\ln[1 + Q] + 2Q \quad (4)$$

where $Q = ([4Bp/T + 1]^{1/2} - 1)/2$, with B equal to the second virial coefficient of the gas. The thermodynamic properties of the Lennard-Jones 12-6 fluid have been carefully simulated by Lotfi *et al.* [26]. Using the values of the vapor pressure of the bulk phase and the expressions for the non-ideality correction to the chemical potential given in Lotfi *et al.*'s paper, one can evaluate the corrections needed to pass from the chemical potential used in the gcmc simulation to the pressure in the adsorption cell. The values given in Table II show the magnitudes of these corrections for the temperatures selected for study and for pressures equal to the vapor pressure of the bulk Lennard-Jones liquid [26]. The second virial correction to μ_{id} was found to be accurate over much of the pressure and temperature range of the simulations to be reported here, but a reasonable all-orders expression is also available [26] when the first order correction is inadequate.

In the Monte Carlo simulation of a system with variable number of particles, one has three kinds of move: displacement, creation and destruction. The relative numbers of these moves

must be optimized to attain equilibrium and give precise average numbers of molecules with appropriate expenditure of computer resources. The fractions of trials devoted to particle displacement, to creation and to destruction amounted to 1/3 each at low densities. As the number of successful trials decreased with increasing adsorbate density, the fraction of displacements was decreased to 20% and the total number of trials was increased.

Preliminary simulations showed that the systems studied could be non-wetting with a nearly first order transition at the bulk vapor pressure or wetting with an isotherm that exhibited rapid variations in the number of particles with pressure as the pressure approached that of the bulk liquid. In such cases, the attainment of equilibrium required large numbers of Monte Carlo trials. Thus for systems not close to the steep regions of the isotherms, the numbers of trials amounted to 0.5 to 2×10^6 for the approach to equilibrium and to 1×10^6 for evaluation of averages after equilibrium had been attained. Different initial states for the Monte Carlo chains were taken, depending upon the expected value of \bar{N} . If \bar{N} was small, either an initially empty box or a configuration from the adjacent isotherm point could be utilized. However, as the system approached the condensation region, the optimum initial state was found to be a box with a uniform density of particles, equal to roughly 0.5 to 0.8 of that for the bulk liquid; as such a system evolved toward equilibrium, a running calculation of the number of particles in the box showed that, aside from fluctuations, it slowly changed in the direction of the eventual equilibrium value. Indeed, the criterion for equilibrium was that this number no longer showed any systematic variation as the number of trials increased. The technique showed quite clearly that much larger numbers of trials were needed to attain equilibrium when the system was in the region of a rapid change in the number of particles with pressure. Consequently, the numbers of trials for these points were 36×10^6 to achieve equilibrium and $6 - 12 \times 10^6$ to generate averages after equilibrium had been reached.

The lateral dimensions L_x, L_y of the box were set at $10 \sigma_{Ne-Ne}$ or 2.78 nm; consequently, the number of atoms held in the box when it is full of liquid is $\simeq 1800$ at the lowest temperature considered. Because of the relatively large volume of this box and the weakness of the adsorption, the correction needed to pass from \bar{N} , the total atoms in the box, to \bar{N}_a , the (thermodynamic excess) number of atoms adsorbed, was non-trivial. One evaluates N_{gas} from the known pressure, the estimated box volume that is accessible to gas atoms, and the temperature and the equation

of state of the bulk. The accessible box volume is estimated from the values of z where the local gas density decreases to zero, and is necessarily inexact because this decrease is not infinitely steep. When the adsorption is quite small, as found for non-wetting systems, the uncertainty in \overline{N}_a , the difference between \overline{N} and N_{gas} , relative to \overline{N} , can be quite significant.

III. ULTRaweak SUBSTRATES

Adsorption isotherms and local densities were simulated for the reduced temperatures listed in Table II. For convenience, the corresponding unreduced temperatures for neon are also listed; they show that the simulations cover the range from a few degrees below the boiling point (27.1 K) up to the vicinity of the critical temperature (44.4 K). For the temperatures listed, the well-depth D was set equal to 16.8, 24, 48, 60, 90, 95, 114, and 120 K in a series of simulations. The theoretical well-depths of Ne vary between 24 K (Cs) and 50 K (Li) for the alkali metals and is 95 K for Mg. The smallest well-depth in the series was based on a previous result for Ne on Cs [35] which is now believed to be too small [10].

Fig. 2 shows adsorption isotherms calculated for $D = 16.8 K$. The discontinuities in all curves at svp indicate that the gas does not wet this surface at any of the temperatures considered, although the decrease in the height of the vertical jump as temperature increase leads one to wonder whether wetting might be present for T^* higher than 1.257 but less than the reduced critical temperature of 1.31. The surface coverages just preceding the jumps are quite small, but difficult to specify in terms of layers adsorbed because the monolayer is poorly defined in such weakly interacting systems. A nominal estimate of the monolayer coverage is $N_{mono} \sim \rho_\ell^{\frac{2}{3}} \mathcal{A} \sim 60$ molecules, based on the bulk liquid density ρ_ℓ and surface area \mathcal{A} .

Note that one can calculate the low coverage parts of these isotherms from Henry's Law, which states that $N_a = pK_H$, with K_H given by:

$$K_H = \frac{\mathcal{A}}{kT} \int [e^{(-U_{gs}(z)/kT)} - 1] dz \quad (5)$$

If the lower limit for z is taken to be $1.2 \sigma_{gs}$ (see Fig. 3), K_H ranges from 0.5 to 0.08 atm^{-1} for the temperatures listed in Table II and $D = 16.8 K$. We see that this expression predicts extremely small numbers of atoms adsorbed, at least for the linear parts of the adsorption isotherms in Fig. 2. The analogous numbers for $D = 120 K$ are 63.0 to 3.3 atm^{-1} .

The key point revealed in Fig. 2 is that neon does not wet a surface with $D = 16.8 \text{ K}$ for all temperatures considered; it is possible that wetting may take place in the small temperature interval between the highest T considered here and T_{cr} , as found experimentally for Rb. [14]. In addition to the isotherms, local densities were evaluated from the simulations for this system. Thus, the density is plotted as a function of z , the distance from the surface, in Fig. 3 for $T^* = 1.148$. The first point to note is that there is a large range of distance for which the densities in all cases are constant and equal to the bulk densities. Furthermore, when the simulation cell is completely filled with liquid, the density profile at the metal surface is not the same as the density at the hard wall despite the ultraweak nature of the adsorbing potential. The second feature is the absence of atoms near both boundary surfaces; this is not surprising for the hard wall boundary, but the behavior near the “adsorbing” surface seems to be the signature of a non-wetting fluid in a container which is otherwise full of liquid. The experiments of Hess *et al.* [14] on Cs have also revealed a region of density depletion near and above the saturated vapor pressure, in qualitative correspondence between this model and the actual Ne/Cs metal system. Based on the available simulation results, we can suggest that the system either undergoes a wetting transition close the critical point, or given the density profiles, it is possible that the system undergoes a drying transition. We are currently trying to simulate this system in the liquid region to see if a drying transition does indeed occur.

Simulated isotherms for $D = 24 \text{ K}$ (corresponding to Ne adsorbed on Cs) were also obtained at the same temperatures as those shown for $D = 16.8 \text{ K}$ and are not significantly different. Results for $D = 48 \text{ K}$ (Ne on Li) are shown in Fig. 4. Here the system appears to be nonwetting for all temperatures studied despite the prediction by Chizmeshya (based on Eq. 1) that Ne should wet Li above 33 K. It is possible that the prewetting regime is so close to saturation that our simulations cannot discern it. Alternately, metastability in this region may be preventing us from obtaining unambiguous results.

IV. STRONGER SUBSTRATES

The gas-solid interaction in the Ne/Mg system is approximated by a well depth $D=95 \text{ K}$ with a wetting temperature of 26 K predicted by the simple surface tension model given in

equation 1 [10]. In this case, the transition is convenient for both experiment and computer simulations (the wetting temperature being far from the critical temperature). Therefore, we explored a range of temperatures around the predicted T_w and found prewetting transitions for temperatures in the predicted range. Fig. 5 shows the simulated adsorption isotherms for the temperatures considered. At $T=21$ K, the adsorption seems to be small up to saturation, while for temperatures between 22 and 29 K prewetting transitions are observed. Thus we estimate $T_w = 22 \pm 1$ K from our simulation data for Mg. This compares favorably with a prediction of 22 K from Eq. 1, using the potential assumed in the simulation. Hence we conclude that the heuristic Eq. 1 works well in this case [36]. It is important to note one fact; the potential used in the simulations is seen in Fig. 1 to have a wider attractive bowl than the ab initio potential of Chizmeshya. Thus we conclude that the best estimate of the wetting temperature on Mg is actually 26 K (as reported in Chizmeshya's paper [10]).

The second important temperature is the prewetting critical temperature. We estimate its value to be 31 K since that is where the isotherms begin to become continuous; this is a provisional value for two reasons. One is that the simulations cannot accurately treat a critical transition, due to size effects. The other is that the potential difference discussed for T_w would imply that 31 K is probably an underestimate relative to what would be predicted with the Chizmeshya potential. Setting aside these concerns, we may compare our results for the reduced prewetting critical temperature, $T_{pw}^* = 0.88$, with the values reported by others for the Ar/CO₂ system. See Table III. Because the D/ϵ ratio for the Ne/Mg and Ar/CO₂ systems are nearly the same, we attribute the differences in the wetting behavior of the two systems to the difference in the width of the potential wells. The width used for the Ne/Mg study is $w = 0.229$ nm while w for the potentials used in the various Ar/CO₂ studies is 0.178 nm. Here "width" means the full width at half minimum of the attractive part of the potential. Increasing the value of w increases the integral, I_v (equation 1). This increase in the left hand side of the equation implies a decrease in the wetting temperature (and the prewetting critical temperature).

The prewetting behavior seen in the Ne/Mg isotherms can also be characterized by its density profiles. In Fig. 6, densities are given for $T=28$ K. The curves shown correspond to density profiles for points on the isotherm immediately before and immediately after the transition at $P = 1.07$ atm. Before the transition, there is little adsorption as the thin film is favored.

However, there is an enhanced density at the surface relative to the gas phase density in the region of attractive potential. This is in sharp contrast to the density profile for the $D=16.8$ K case where the density of the fluid in most of the simulation box is equal to the gas phase density (See Fig. 3). After the transition, three distinct peaks can be seen in the density profiles, indicating that the prewetting behavior corresponds to a transition from less than a monolayer to about 2.5 to 3 layers; the total coverage jump 20 is a factor of 15. The separation between the peaks close to the surface is $0.93 \sigma_{gg}$ for the the first two and $0.98 \sigma_{gg}$ between the second and third peaks. The spacing between close-packed (111) planes of bulk Ne is $0.261 \text{ nm} = 0.94 \sigma_{gg}$.

In order to see the dependence of the adsorption and wetting properties upon gas-solid interaction strength, we have simulated adsorption for several other values of D while holding the temperature fixed. Fig. 7 shows isotherms at a high temperature (39 K) for some values of D considered while Fig. 8 gives similar results for a lower temperature ($T = 28$ K). At the high temperature, the curves for 90 and 120 K show the smooth increase of coverage with pressure as one approaches the saturated liquid, but that for 60 K is sharply different. At first glance, the apparent discontinuity in slope appears to be the signal of a non-wetting surface, but the fact that the jump in coverage occurs at a pressure slightly less than that of the saturated liquid actually indicates a prewetting transition. Furthermore, the local densities that are plotted in Fig. 9 for the 60 K system show peaks close to the adsorbing surface which are due to monolayer formation. As noted above and in other simulation studies of wetting [23,37], these peaks will generally be absent for the condensate formed in non-wetting systems. One also observes in Fig. 9 that the density fluctuations in the monolayer region are smaller than those farther away, at $z > 5 \sigma$. This behavior is consistent with the following argument. In a slowly varying system, the number fluctuation ΔN within a very small volume will satisfy the theorem known to apply to a uniform system:

$$\langle (\Delta N)^2 \rangle = kT \frac{dN}{d\mu} \quad (6)$$

where the derivative is that of a uniform system at the local density, with a chemical potential value shifted from that of the nonuniform system by the net external potential. This is an application of so-called “local thermodynamics”. For qualitative purposes, and often quantitative

ones, one may apply this approach to the highly nonuniform vicinity of the monolayer. Here one finds a much smaller density fluctuation for the (quite intuitive) reason that the derivative in that region is much smaller than for larger z ; the monolayer density profile does not change much with the addition of particles at larger z .

For the low temperature study the pressures for the prewetting transition are shifted to lower pressures relative to the bulk vapor pressure. Thus, isotherms at 28 K clearly exhibit the complete range of wetting behavior as the well-depth is varied from 95 K to 114 K. At $D=60$ K (not shown), the system is nonwetting, while at $D=114$ K the adsorption is continuous, with prewetting transitions occurring for systems of intermediate strengths. Unfortunately, the fluctuations in the transition regions are larger at this temperature and for well-depths below 95 K we have not obtained results in the transition region that were sufficiently precise to give us a good prediction of the transition pressure. However, the fact that there are large fluctuations is a good indicator that a first order transition is taking place. In the continuous and non-wetting regions at this temperature, no such problems occurred.

Finally, we look to see what happens if we modify the potential to take into account the corrugation in the surface. We constructed a potential by adding Ne-Mg pair interactions, assuming a Mg surface with a simple cubic structure (lattice parameter of .401 nm) and chose a well-depth for this potential such that the well-depth of the lateral average of the corrugated potential is identical to that of the smooth potential. The potentials are compared in Fig. 10 and the resulting isotherms are shown in Fig. 11. The periodicity causes a shift in the pressure at which the prewetting transition occurs and therefore brings about a lowering of the wetting temperature. This is presumably due to the deeper potentials at the adsorption sites, but other factors (such as the lateral spacing of adsorbent atoms) could play a role in this phenomenon [38]. The density distributions which correspond to coverages immediately before and immediately after the prewetting transition are given in Fig. 6 for the flat surface and in Fig. 12 for the corrugated potential model. These plots are very similar, indicating that the nature of the transition has remained the same despite the increased corrugation. The principal difference is a $\sim 60\%$ higher film density just below the transition in the corrugated surface case.

V. SUMMARY

In this paper we have examined the nature of the wetting transition of Ne on various weakly adsorbing surfaces. For the case of the most inert surface, Cs, we find negligible adsorption of Ne throughout the temperature range explored. In fact, for pressures (slightly) above saturated vapor pressure, we find evidence of a dry region near the surface. This behavior is qualitatively similar to what was found experimentally by Hess, Sabatini, and Chan. In the case of somewhat more attractive surfaces, e.g. Mg, we find evidence of a prewetting regime of temperature. The adsorption there is characterized by a jump in coverage at a specific pressure near, but below, saturation. The coverage changes by a factor of order five to fifteen at this transition. This finding is consistent with both experiments (inert gases on alkali metal surfaces and Hg on sapphire) and with general trends established in the simulations of Monson and coworkers.

While there is every indication that this prewetting transition behavior is generic on weakly attractive surfaces, more extensive study is needed to assess the criteria for the prewetting phenomenon. One useful guide to its occurrence is the simple model, Eq. 1, which predicts the wetting temperature from the potential and the bulk fluid's properties. This was found to work surprisingly well for the case of Mg, but for the Li surface, the results are ambiguous. The simple dependence contained in that relationship implies that one may invert the wetting transition temperature obtained experimentally in order to deduce an integral property of the potential. This capability can be particularly useful in circumstances where the gas-surface attraction is weak, because then the Henry's law regime of low coverage may be inaccessible or difficult to utilize as a means of analyzing the potential.

We have found qualitatively similar results for the cases of a smooth adsorption potential and a corrugated potential (similar to what might occur on a Mg surface). It is not surprising that the effect of the periodic potential is small at the transition pressure because most of the adsorbate lies in the region of negligible corrugation and the amplitude of the Fourier components of the potential are $< kT$ at the potential minimum.

The prewetting transition has thus far been investigated in relatively few adsorption systems. We hope that our conceptually straightforward findings encourage experimentalists to extend their studies to other adsorption systems which are weak-binding systems. Some of these other

cases have rough estimates of wetting temperatures presented by Chizmeshya *et al.*

In future publications we would like to explore two problems of further interest. In one, we will report results of a study of the effects of roughness on the wetting transition. We hope at a later date to evaluate the temperature regime close to the critical point where wetting transitions have been found for Ne on Rb and Cs.

ACKNOWLEDGMENTS

We are most grateful to Victor Bakaev for sharing his expertise in Monte Carlo simulations and for helpful discussions. We are also grateful to George Hess, Moses Chan and Ian McDonald for stimulating conversations. This research was supported by the National Science Foundation. We are especially grateful to *Fondazione Aldo Ing. Gini* for the generous support of Ing. S. Curtarolo.

TABLES

TABLE I. Potential ratios

The ratio D^* of the adsorption potential well depth D to a nominal pair potential well depth ϵ (in parentheses, in Kelvin) is tabulated for simple gases on various surfaces. Pair well depths are taken from reference [13], except for the case of H_2 , which is taken from Cheng *et al.* [12] and Ne, which is fit to the bulk critical temperature (44.4K). Adsorption well depths are from Chizmeshya *et al.* [10] except Au [12] and CO_2 [4].

	He (10.22)	Ne (33.9)	H_2 (34.3)	Ar (119.8)
Au	8.5	8.3	13	8.2
Mg	3.4	2.8	5.5	3.5
Li	1.7	1.5	2.8	2.0
Rb	0.72	0.71	1.1	1.1
Cs	0.68	0.70	1.1	1.1
CO_2	—	—	—	2.64

TABLE II. Parameters of the simulations
(Here, σ denotes liquid-vapor equilibrium)

T^*	T (K) (L.J. neon)	p_σ (atm) (L.J. neon)	$e^{(\mu_{real}-\mu_{id})\sigma/kT}$ (all orders)	$e^{(\mu_{real}-\mu_{id})\sigma/kT}$ (second virial)
0.656	22	0.1424	0.9889	0.989
0.738	25	0.4828	0.9725	0.973
0.812	28	1.2249	0.9478	0.948
0.902	31	2.5788	0.9154	0.915
1.011	34	5.7238	0.862	0.862
1.093	37	9.4306	0.817	0.815
1.148	39	12.7238	0.784	0.777
1.230	42	19.0158	0.732	0.714
1.257	43	21.5500	0.716	0.692

TABLE III. Wetting temperatures for Ne/Mg and Ar/CO₂ studies.

Source	T_w^*	T_{pw}^*
Ebner and Saam [4]	0.77	0.92
Evans and Tarazona [33]	0.957	0.988
Meister and Kroll [34]	0.90	
Finn and Monson [19]	0.84	0.94
Sokołowski and Fischer [21]	0.975 ± 0.025	
This work	0.65	0.88 ± 0.03

REFERENCES

- [1] S. Dietrich, in *Phase Transitions and Critical Phenomena*, ed. C. Domb and J. L. Lebowitz, (Academic, London, 1988) Vol. 12, p. 1; P. G. de Gennes, Rev. Mod. Phys. **57**, 827 (1985); Bob Evans and Moses Chan, Physics World **9**, #4, 48 (1996).
- [2] R. Pandit, M. Schick, and M. Wortis, Phys. Rev. B **26**, 5112, (1982).
- [3] J. W. Cahn, J. Chem. Phys. **66**, 3667 (1977).
- [4] C. E. Ebner and W. F. Saam, Phys. Rev. Lett. **38**, 1486 (1977).
- [5] J. Rutledge and P. Taborek, Phys. Rev. Lett. **69**, 937 (1992).
- [6] P.-J. Nacher and J. Dupont-Roc, Phys. Rev. Lett. **67**, 2966 (1991); K. S. Ketola, S. Wang, and R. B. Hallock, Phys. Rev. Lett. **68**, 201 (1992).
- [7] E. Cheng, M. W. Cole and W. F. Saam and J. Treiner, Phys. Rev. Lett. **67**, 1007 (1991); Phys. Rev. B **46**, 13967 (1992); Erratum B **47**, 14661 (1993).
- [8] E. Cheng, G. Mistura, H. C. Lee, M. H. W. Chan, M. W. Cole, C. Carraro, W. F. Saam and F. Toigo, Phys. Rev. Lett. **70**, 1854 (1993).
- [9] G. Mistura, H. C. Lee and M. H. W. Chan, J. Low Temp. Phys. **96**, 221 (1994); D. Ross, P. Taborek and J.E. Rutledge, to be published.
- [10] A. Chizmeshya, M. W. Cole, and E. Zaremba, J. Low Temp. Phys. **110**, 677 (1998).
- [11] G. Vidali, G. Ihm, H. Y. Kim and M. W. Cole, Surface Science Repts. **12**, 133 (1991).
- [12] E. Cheng, M. W. Cole, W. F. Saam and J. Treiner, Phys. Rev. B **48**, 18214 (1993).
- [13] R. O. Watts and I. J. McGee, *Liquid State Chemical Physics*, (Wiley, New York, 1976).
- [14] G. B. Hess, M. J. Sabatini and M. H. W. Chan, Phys. Rev. Lett. **78**, (1997).
- [15] V. F. Kozhevnikov, D. I. Arnold, S. P. Naurzakov, and M. E. Fisher, Phys. Rev. Lett. **78**, 1735 (1997).
- [16] F. Hensel and M. Yao, Eur. J. Sol. Stat. Inorg. Chem. **34**, 861 (1997)).

[17] A partial and preliminary report of this research appeared as M. J. Bojan, M. W. Cole, J. K. Johnson, W. A. Steele, and Q. Wang, *J. Low Temp. Phys.* **110**, 653 (1998).

[18] Q. Wang and J. K. Johnson, *Fluid Phase Equilib.* **132**, 93 (1997); Q. Wang, J. K. Johnson and J. Q. Broughton, *J. Chem. Phys.* **107**, 5108 (1997).

[19] J. E. Finn and P. A. Monson, *Phys. Rev. A* **39**, 6402 (1989).

[20] Y. Fan and P. A. Monson, *J. Phys. Chem.* **99**, 6897 (1993).

[21] S. Sokołowski and J. Fischer, *Phys. Rev. A* **41**, 6866 (1990).

[22] M. J. P. Nijmeijer, C. Bruin, A. F. Bakker, and J. M. J. Leeuwen, *Mol. Phys.* **72**, 927 (1991).

[23] J. H. Sikkenk, J. O. Indekeu, J. M. J. van Leeuwen and E. O. Vossneck, *Phys. Rev. Lett.* **59**, 98 (1988).

[24] J. H. Sikkenk, J. O. Indekeu, J. M. J. van Leeuwen, E. O. Vossneck, and A. F. Baker, *J. Statist. Phys.* **52**, 23 (1988).

[25] B. Smit, *J. Chem. Phys.* **96**, 8639 (1992).

[26] A. Lotfi, J. Vrabec and J. Fischer, *Mol. Phys.* **76**, 1319 (1992).

[27] L. W. Bruch, M. W. Cole, and E. Zaremba, *Physical Adsorption: Forces and Phenomena* (Oxford Press, Oxford, 1997).

[28] W. A. Steele, *J. Phys. Chem.* **82**, 817 (1978).

[29] The decay length is $2\pi\sqrt{8Wm}/h$, where W and m are the electronic work functions and mass.

[30] M. P. Allen and D. J. Tildesley, *Computer Simulation of Liquids* (Clarendon, Oxford, 1987).

[31] D. Frenkel and B. Smit, *Understanding Molecular Simulation* (Academic Press, San Diego, 1996).

[32] D. Nicholson and N. G. Parsonage, *Computer Simulation and the Statistical Mechanics of*

Adsorption, (Academic Press, New York, 1982).

- [33] P. Tarazona and R. Evans, Phys. Rev. A **28**, 1864 (1983).
- [34] T. F. Meister and D. M. Kroll, Phys. Rev. A **31** 4055 (1985).
- [35] E. Zaremba and W. Kohn, Phys. Rev. B **15**, 1769 (1977).
- [36] Similar good agreement is reported by Cheng *et al.*, [8].
- [37] P. Adams and J. R. Henderson, Mol. Phys. **73**, 1383 (1991).
- [38] We are currently working on this problem.

FIGURES

FIG. 1. Summed 10-4 potential (—) used in this study is compared to the integrated 9-3 potential for the interaction of Ne with alkali and alkaline earth metals (— —) and the 9-3 potential for the Ar/CO₂ interaction (· · ·). For the 10-4 potential, z_{min} is 0.497 nm, while for the integrated potentials, z_{min} is the distance above the jellium edge, and is 0.307 nm for the Ne/metal potential, and 0.320 nm for the Ar/CO₂ potential.

FIG. 2. Adsorption isotherms for a Lennard-Jones gas (Ne) on a model Rb surface with gas-solid interaction well-depth $D = 16.8$ K. Shown are isotherms for T=43 K (○ and —), T=42K (* and — —), T=41 K (△ and — · —), T=39 K (□ and — —), T=37 K (▲ and — —), T=34 K (● and —) and T=32 K (■ and — · —).

FIG. 3. Local densities for the gas in the computer box for the system of Fig. 2 at $T^* = 1.148$. The area of this box is $.773 \text{ nm}^2$ and the density gives the total number of atoms per unit volume in the box as a function of distance from the surface. For each curve, the number of adsorbed atoms (= total atoms minus gas atoms in a box of volume V at a pressure p) in the box is denoted by N_a . Pressures are 13.5 atm at $N_a/\mathcal{A}=11.1 \text{ nm}^{-2}$ (—) 13.9 atm at $N_a/\mathcal{A}= 137 \text{ nm}^{-2}$ (· · ·) and 16.5 atm at $N_a/\mathcal{A}=183 \text{ nm}^{-2}$ (— · —). Bulk liquid and gas densities at the adsorption pressures for each curve are shown by the horizontal lines. The simulation value of the vapor pressure of neon at $T^*=1.148$ is given in Table I.

FIG. 4. Adsorption isotherms for a Lennard-Jones gas (Ne) on a model Li surface with gas-solid interaction well-depth 48 K. The temperatures are 43 K (× and — —), 42 K (○ and —), 39 K (* and — —), 37 K (△ and — · —), 34 K (□ and — —), 32 K (▲ and — —), 28 K (● and —) and 25 K (■ and — · —). The vertical lines represent the saturated vapor pressure at the respective temperatures.

FIG. 5. Adsorption isotherms for Ne on a model Mg surface with gas-solid interaction well-depth $D = 95$ K. The corresponding temperatures are 31 K (□ and — —), 29 K (▲ and — —), 28 K (● and —), 27 K (■ and — · —), 25 K (○ and — · —), 23K (* and — —), 22 K (△ and — · —), and 21K (× and — —). The vertical lines represent the saturated vapor pressure at the respective temperatures.

FIG. 6. Local densities as a function of the reduced distance from the surface for the gas in the model Ne/Mg system ($D = 95K$) at $T=28$ K. Curves shown are for coverages of 22. atoms/nm³ at $P = 1.04$ atm (—) and 303. atoms/nm³ at $P = 1.05$ atm (···). The bulk liquid density (— —) and the gas density (− · −) are represented for comparison.

FIG. 7. Adsorption isotherms for a Lennard-Jones gas (Ne) at $T^* = 1.148$ on several surfaces with the interaction well-depths $D=16.8$ K (■ and − · −), $D=60$ K (● and —), $D=90$ K (▲ and − −) and $D=120$ K (□ and — —). The prewetting jump for $D=60$ K goes from $N_a/\mathcal{A} = 17.9$ molecules/nm² to $N_a/\mathcal{A} = 102.7$ molecules/nm².

FIG. 8. Adsorption isotherms at $T=28$ K for model systems with gas-solid interaction strengths slightly different from the model Ne/Mg system. Shown are isotherms corresponding to well-depths of 95 K (■ and —, corresponding to Ne/Mg), 102 K (● and − −), 108 K (□ and — —), 114 K (○ and − · −).

FIG. 9. Same as Fig. 3, but for an interaction well-depth of 60 K. Pressures are 13.0 atm at $N_a/\mathcal{A}=14.5$ nm^{−2}, 13.5 atm at $N_a/\mathcal{A}= 92.8$ nm^{−2}, 13.9 atm at $N_a/\mathcal{A}=152$ nm^{−2}, and 14.2 atm at $N_a/\mathcal{A}=170$ nm^{−2}.

FIG. 10. Reduced gas-solid adsorption potentials as a function of reduced distance from the surface for a continuum flat surface (■, modeling Ne/Mg), and for a corrugated surface with a square lattice (lattice constant $a=.401$ nm). In this last case, the adatom is placed vertically above three sites: S(—), SP (— —), and A (− · −) whose location is indicated in the inset.

FIG. 11. Adsorption isotherms at $T= 28$ K for the Ne/Mg model system in the case of a continuum flat surface (■ and − −) and a corrugated surface (□ and · · ·).

FIG. 12. Same as Fig. 6 but for the corrugated potential. The two isotherm points that were considered are for coverages of 34. atoms/nm³ at $P = 0.92$ atm (—) and 289. atoms/nm³ at $P = 0.94$ atm (− −).

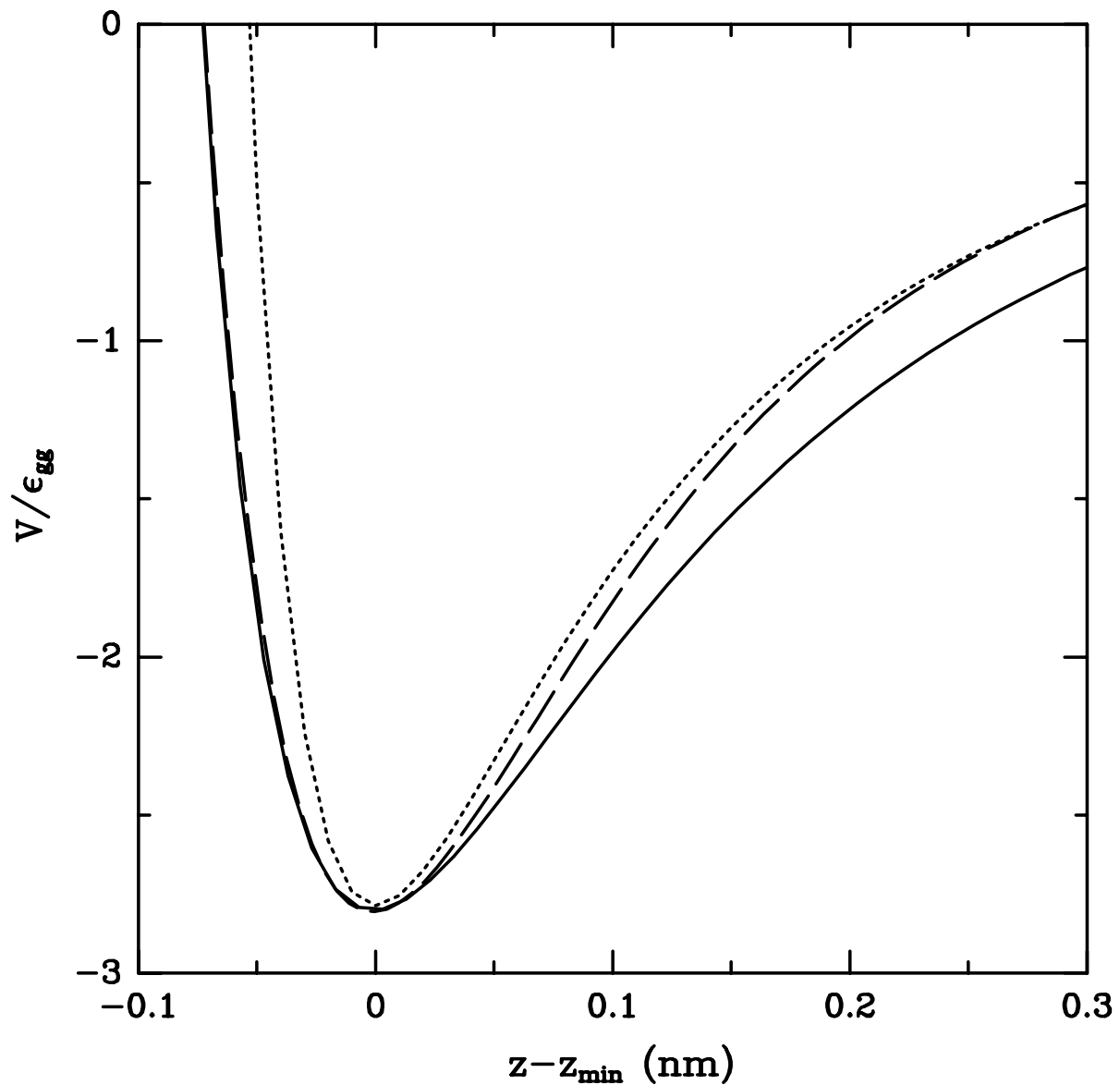


FIG. 1

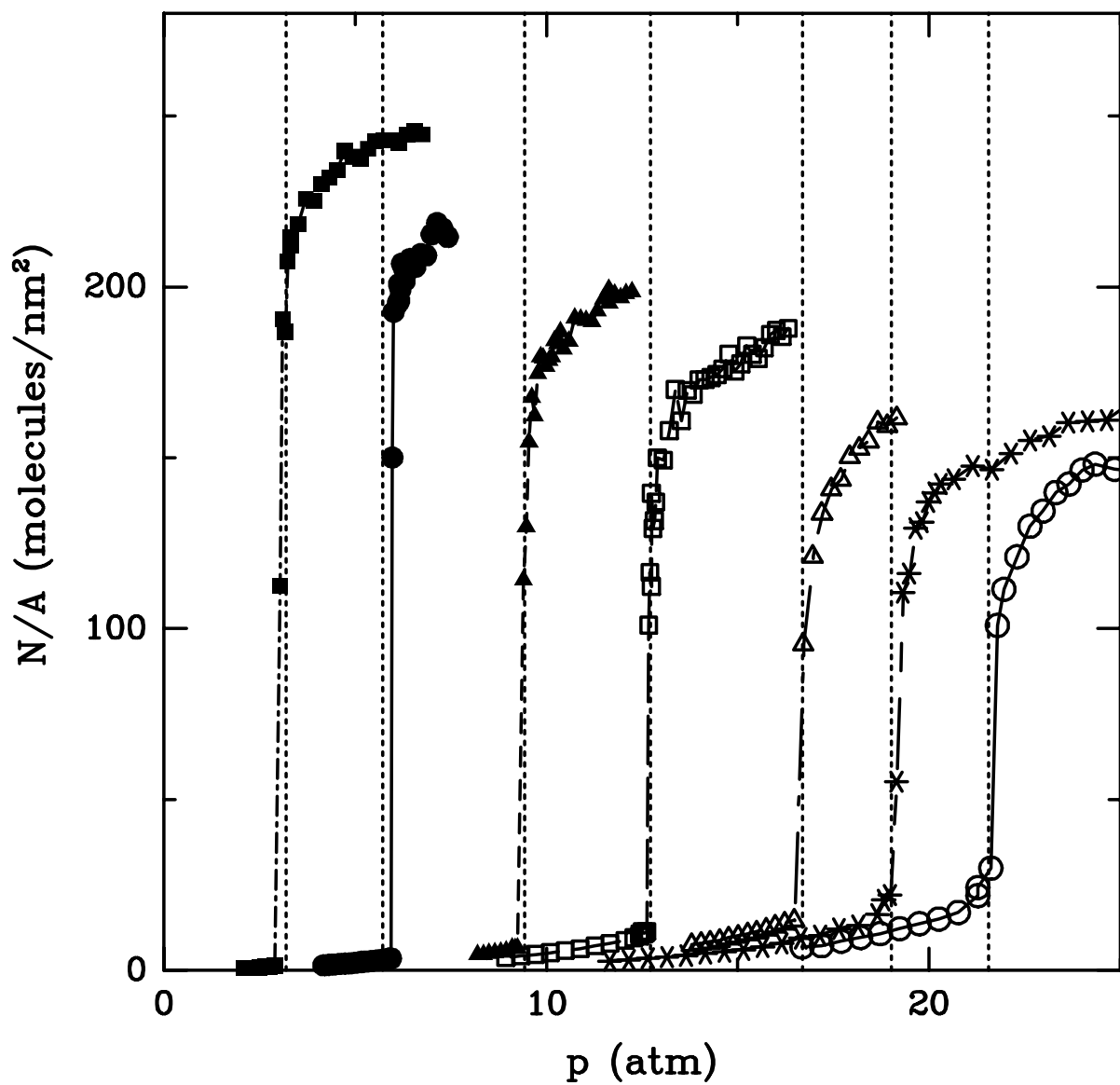


FIG. 2

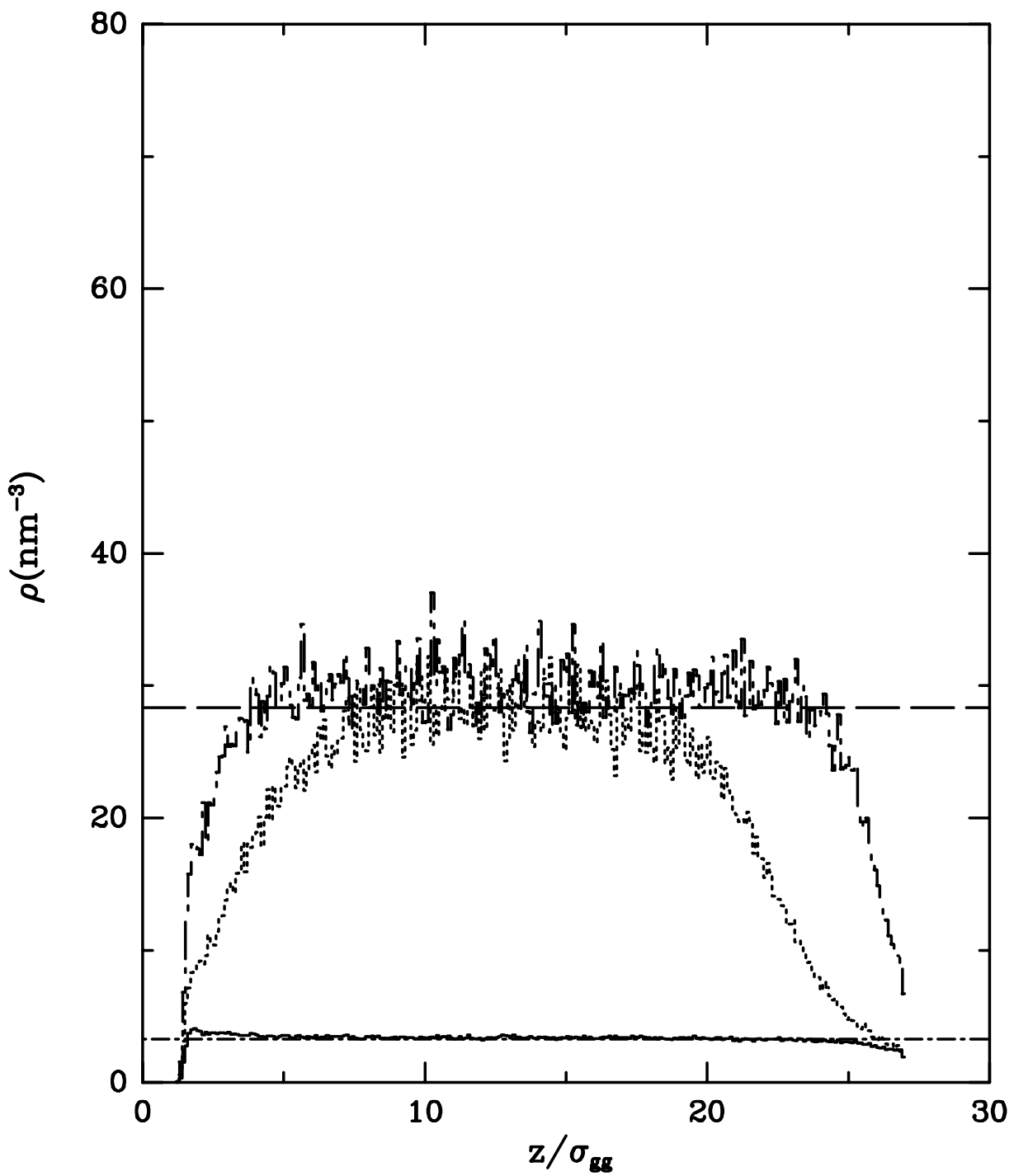


FIG. 3

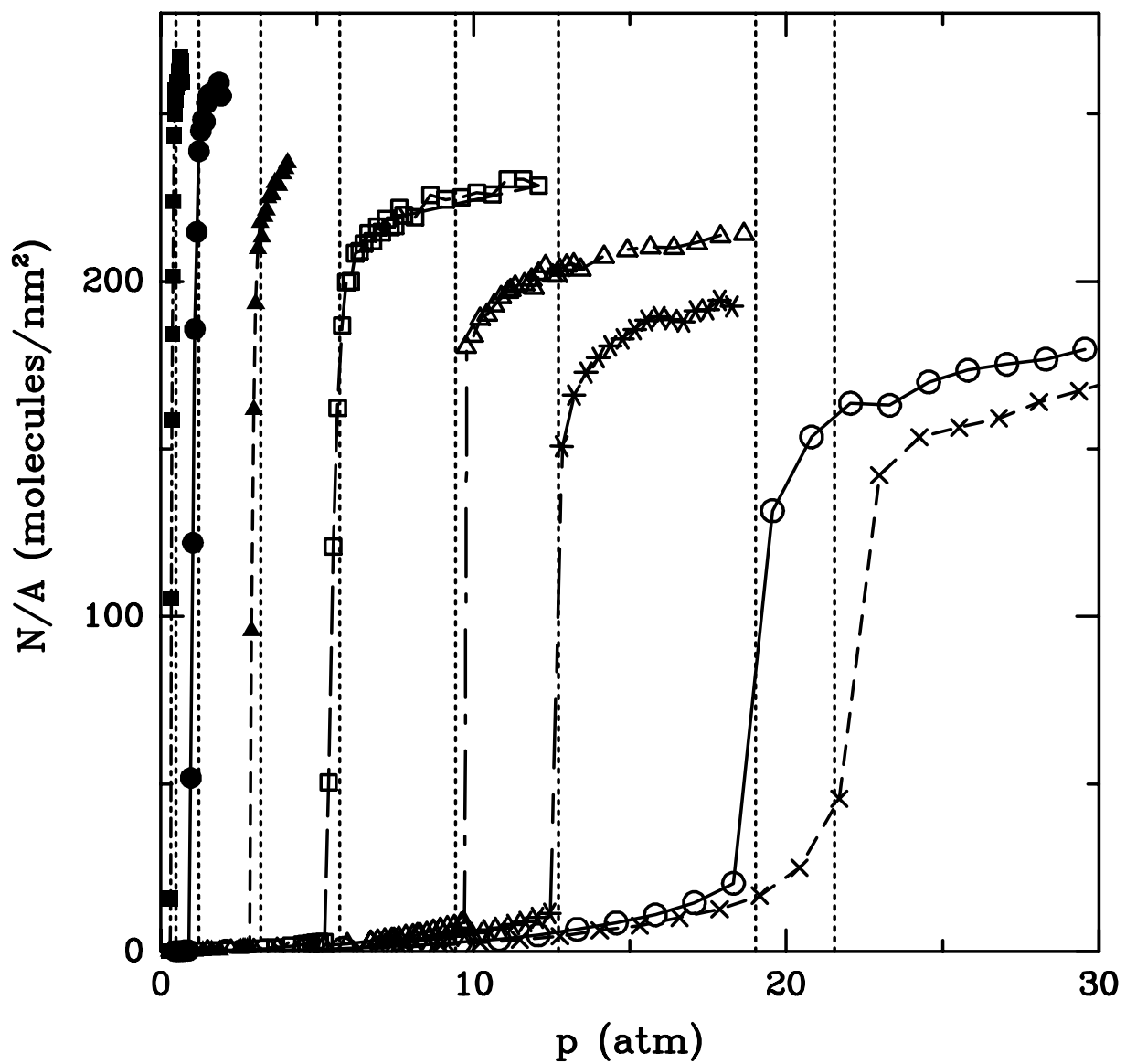


FIG. 4

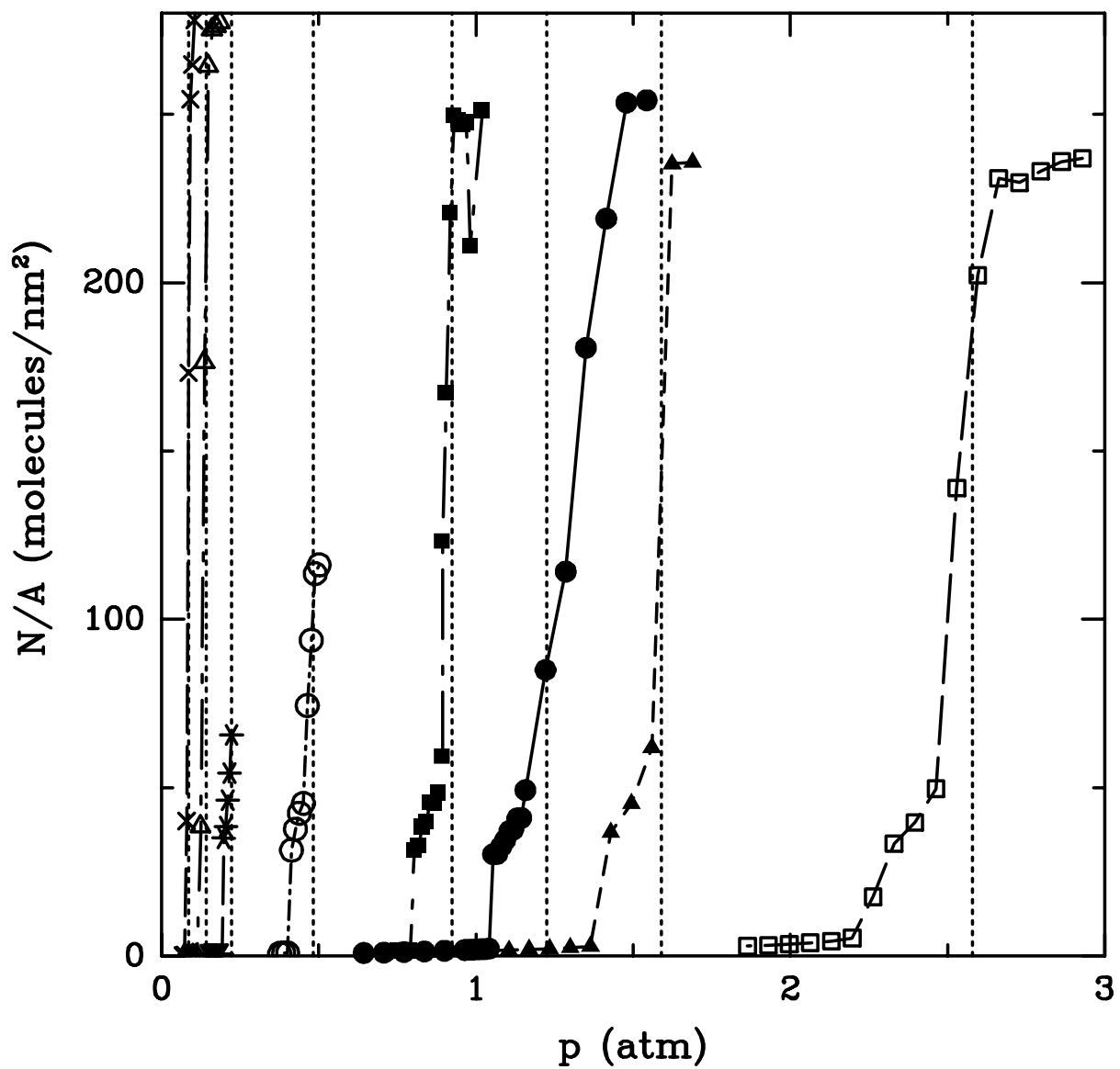


FIG. 5

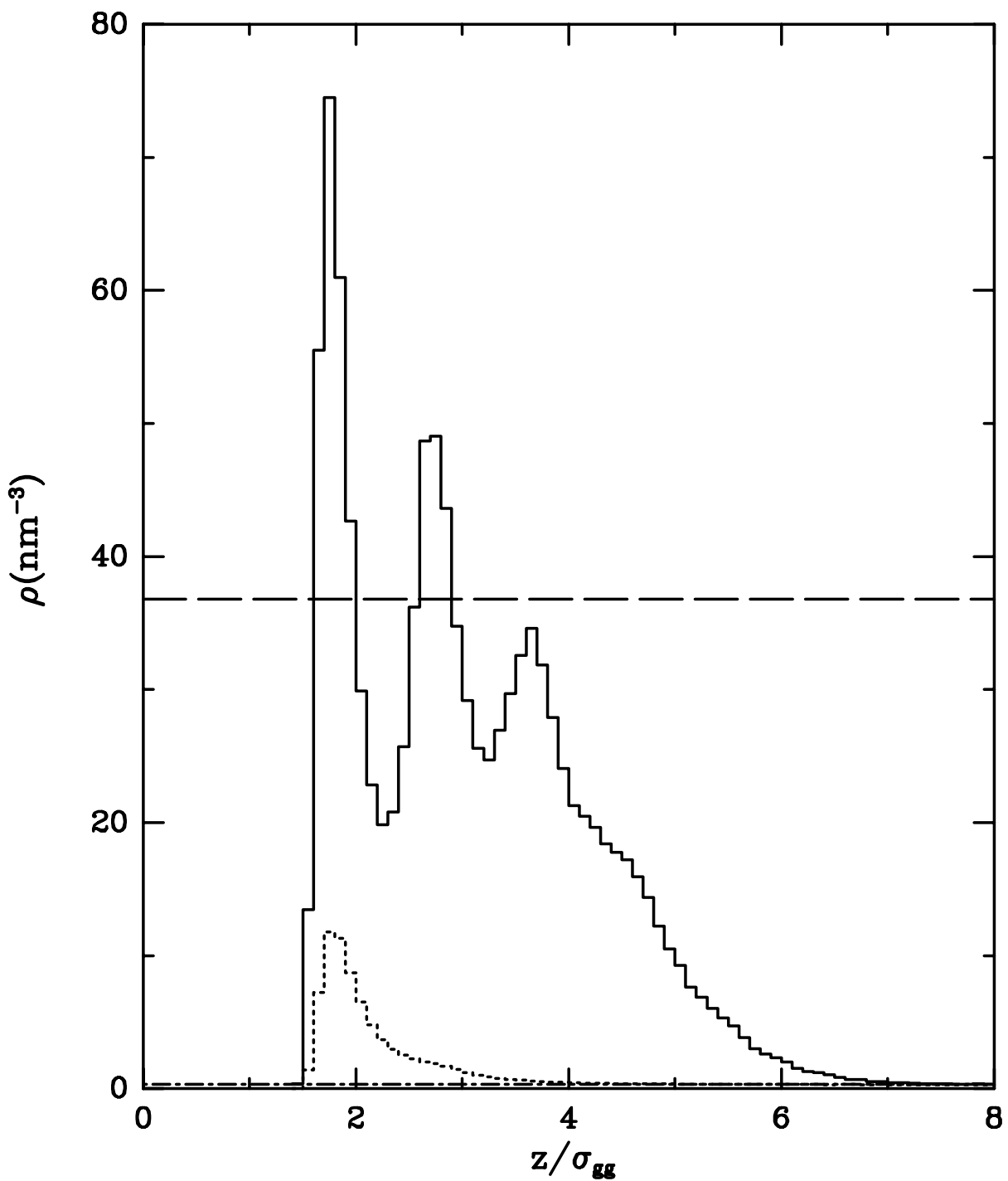


FIG. 6

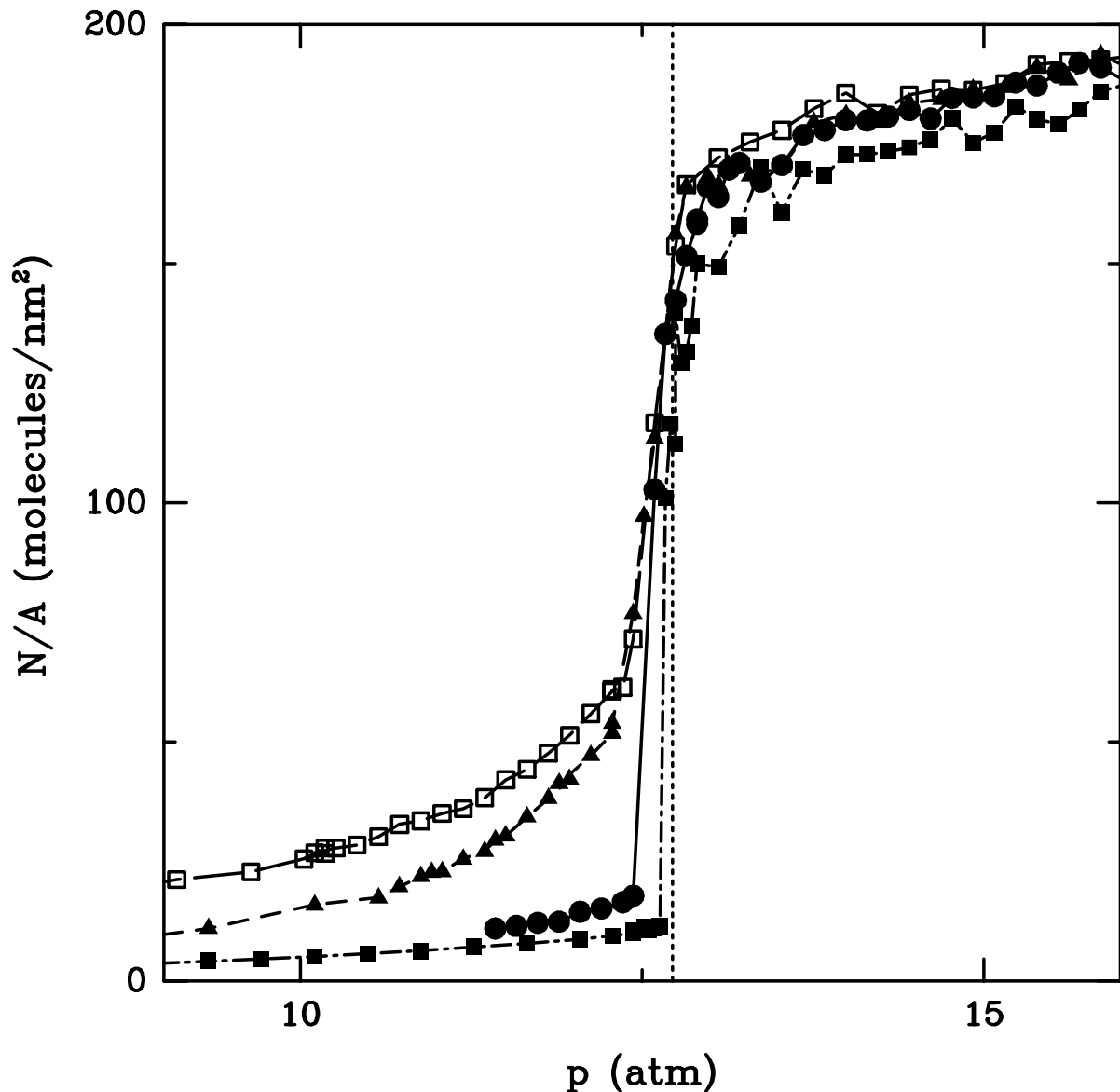


FIG. 7

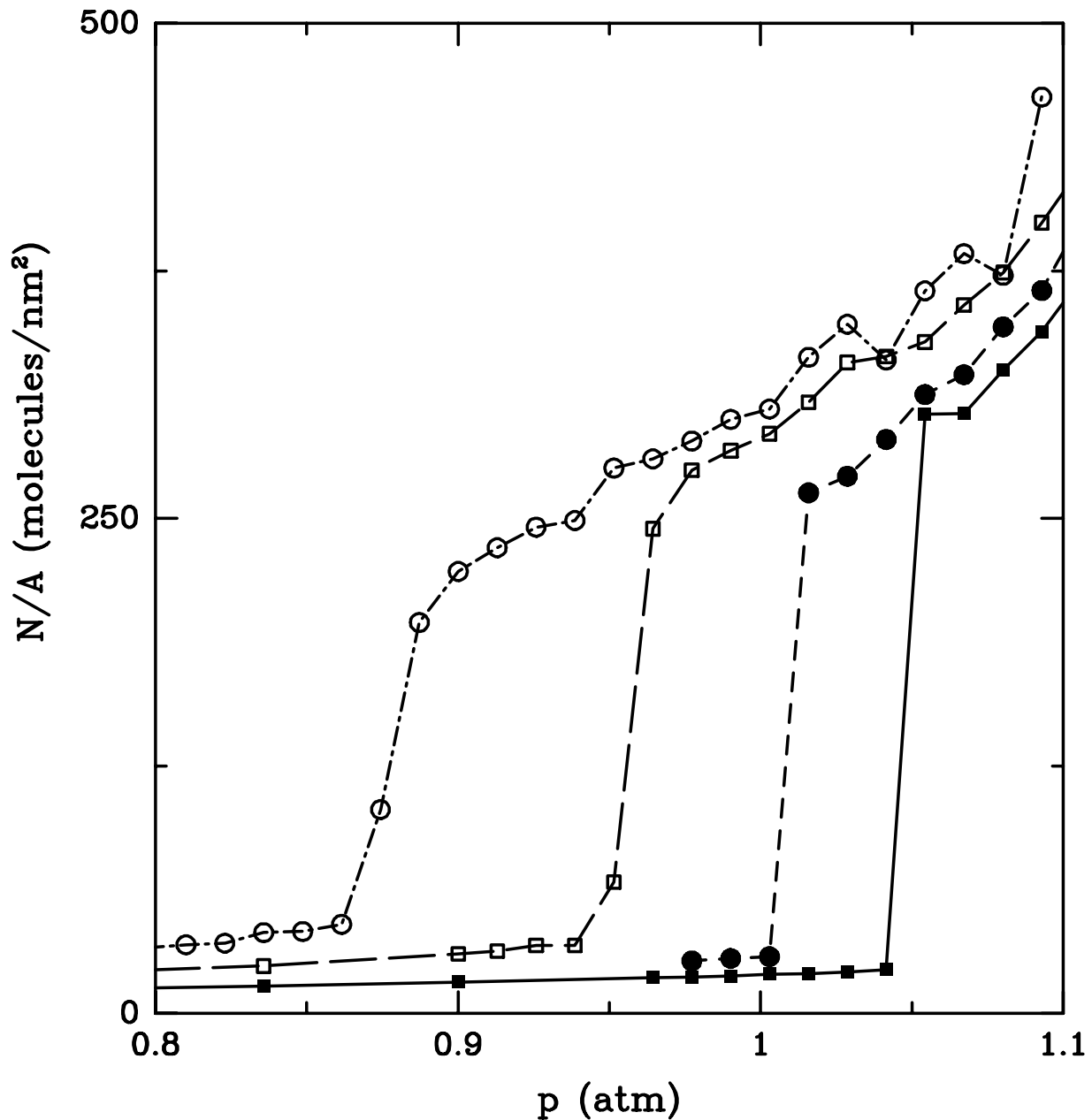


FIG. 8

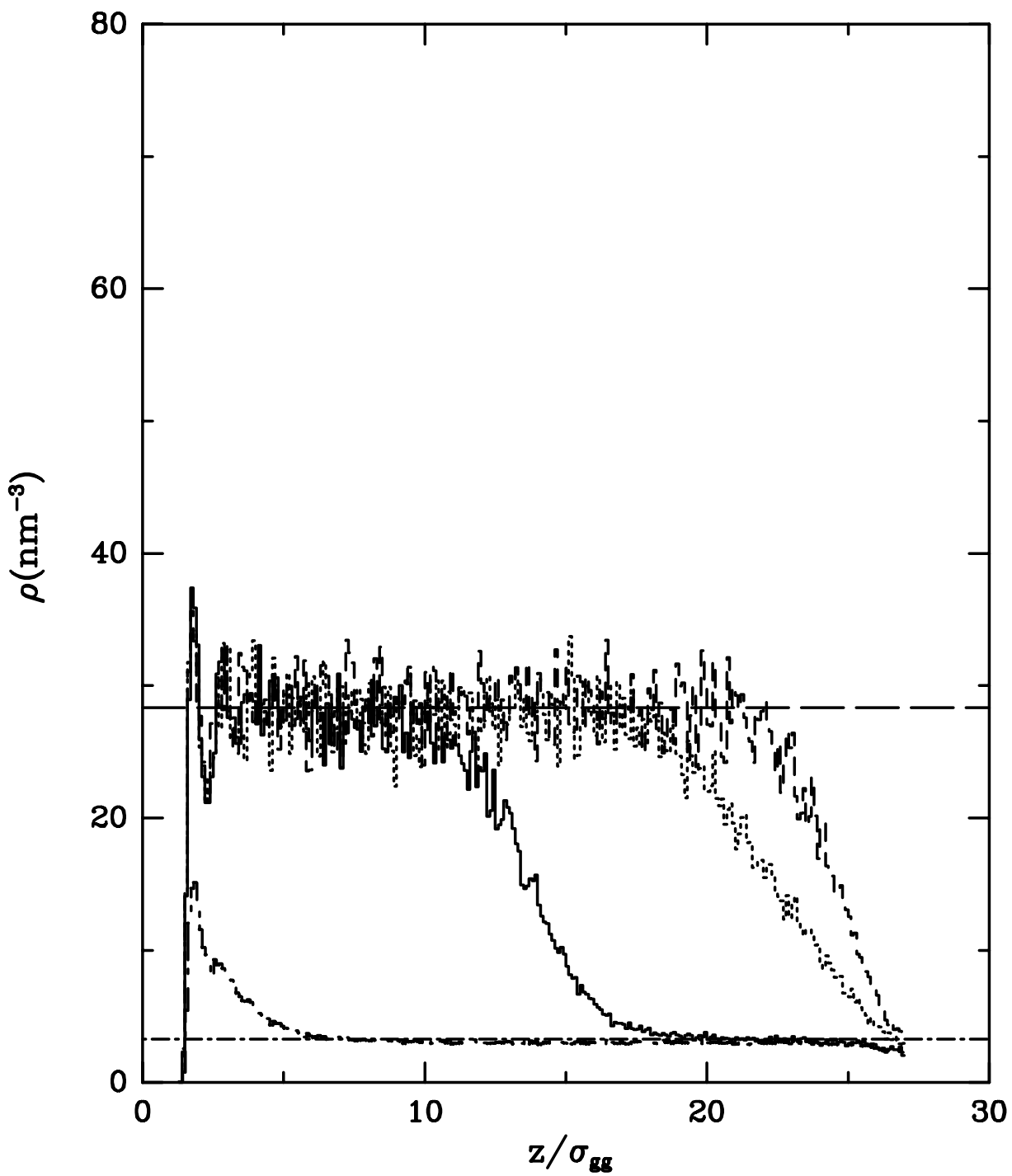


FIG. 9

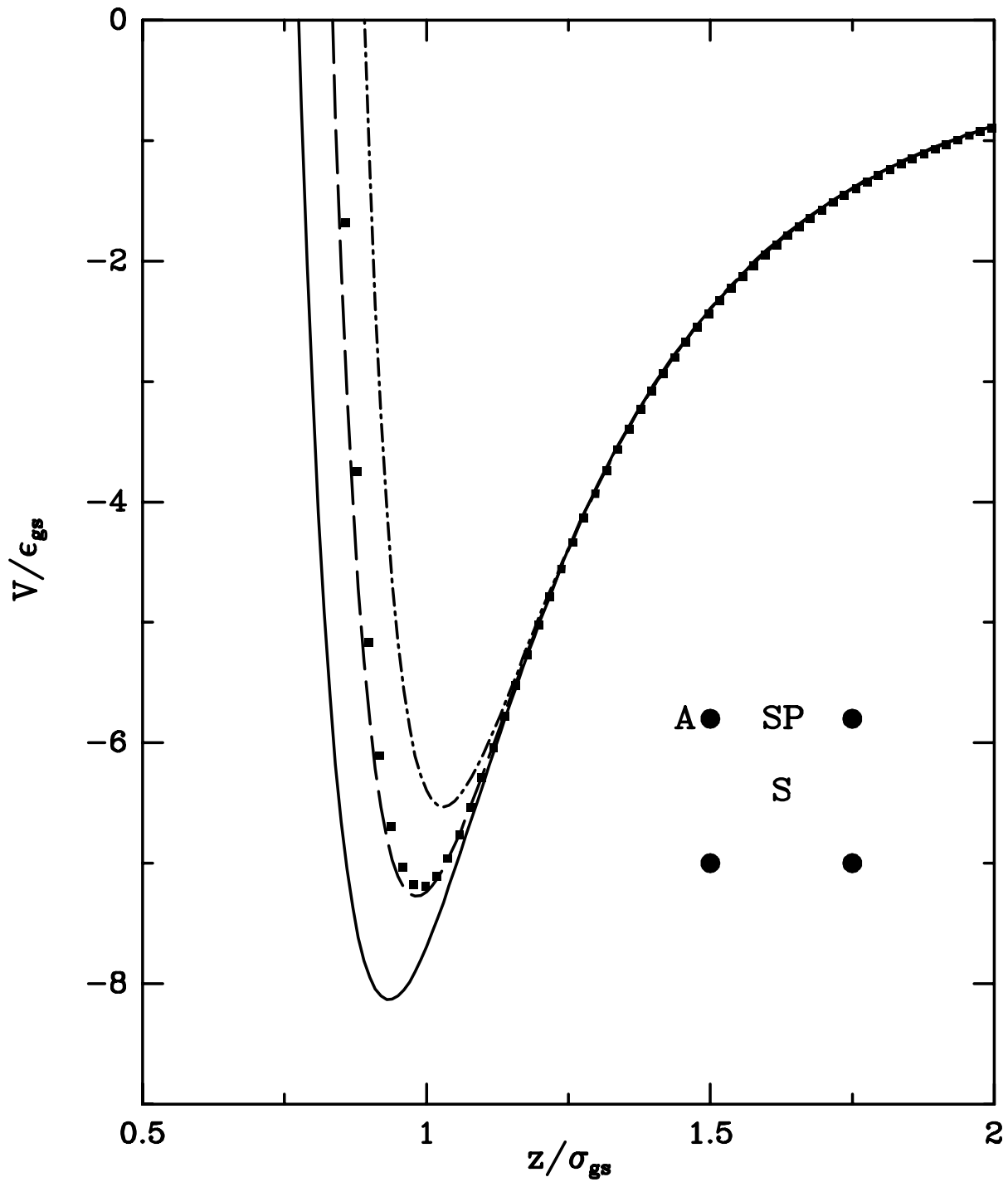


FIG. 10

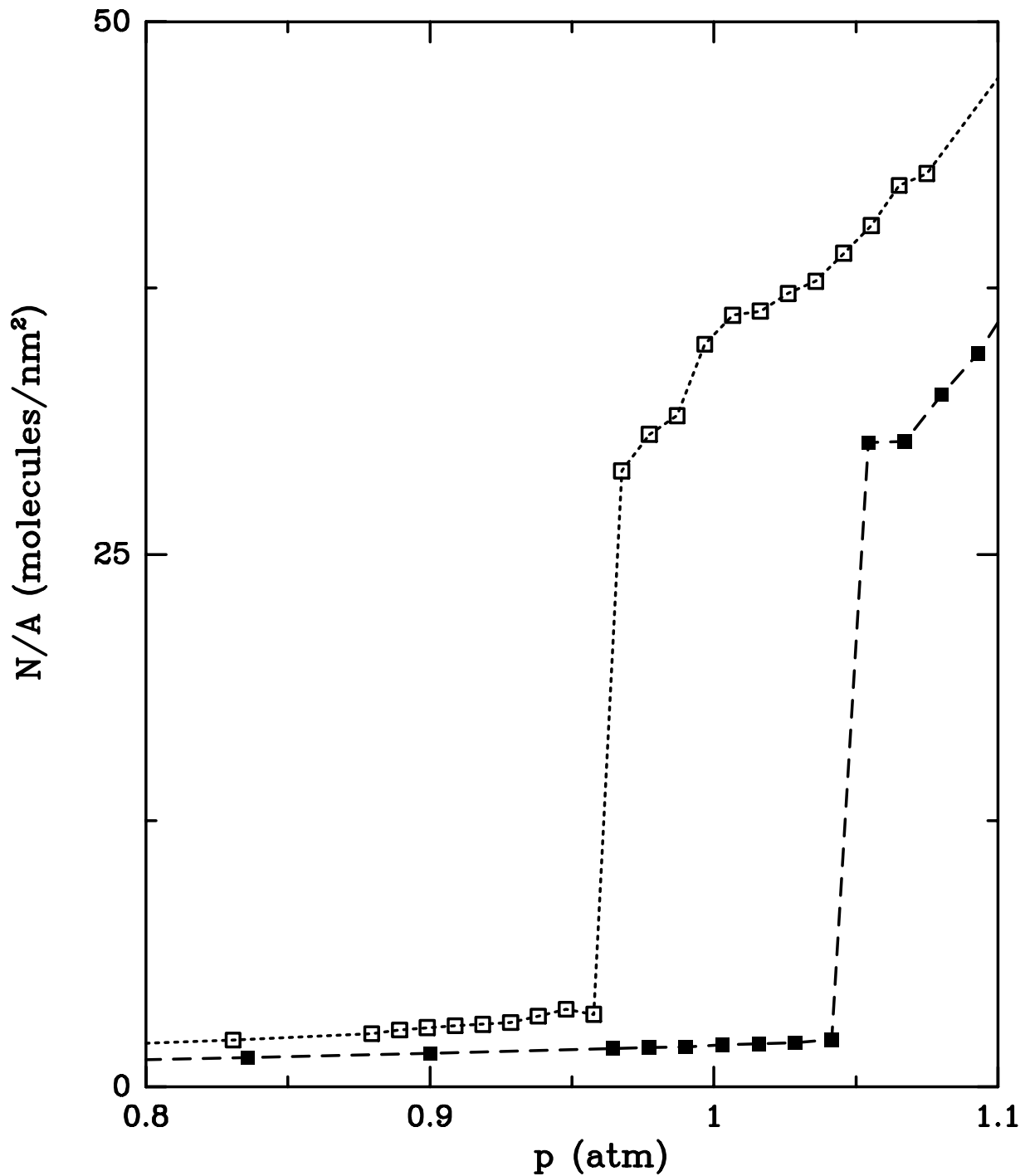


FIG. 11

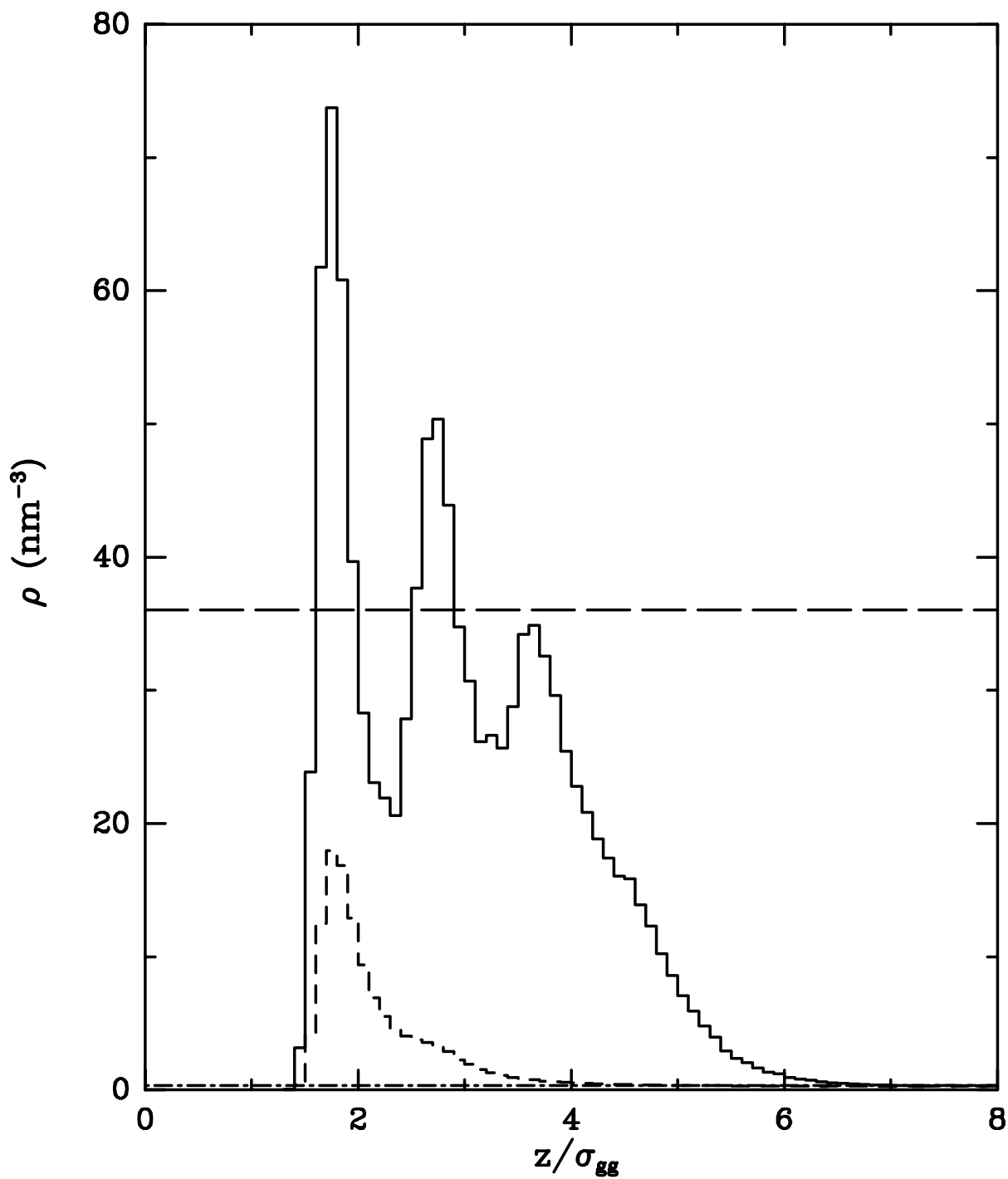


FIG. 12